

On the Stability of Undesirable Equilibria in the Quadratic Program Framework for Safety-Critical Control

Matheus F. Reis and A. Pedro Aguiar

Abstract—Control Lyapunov functions (CLFs) and Control Barrier Functions (CBFs) have been used to develop provably safe controllers by means of quadratic programs (QPs). This framework guarantees safety in the form of trajectory invariance with respect to a given set, but it can introduce undesirable equilibrium points to the closed loop system, which can be asymptotically stable. In this work, we present a detailed study of the formation and stability of equilibrium points with the QP framework for a class of nonlinear systems. We introduce the useful concept of compatibility between a CLF and a family of CBFs, regarding the number of stable equilibrium points other than the CLF minimum. Using this concept, we derive a set of compatibility conditions on the parameters of a quadratic CLF and a family of quadratic CBFs that guarantee that all undesirable equilibrium points are not attractive. Furthermore, we propose an extension to the QP-based controller that dynamically modifies the CLF geometry in order to satisfy the compatibility conditions, guaranteeing safety and quasi-global convergence of the system state to the CLF minimum. Numeric simulations illustrate the applicability of the proposed method for safety-critical, deadlock-free robotic navigation tasks.

Index Terms—Lyapunov methods, Control barrier functions

I. INTRODUCTION

THE engineering of *safety-critical systems* is a fruitful and rich topic receiving a growing amount of attention nowadays. Safety-critical systems are of crucial importance for many industrial sectors and production lines, where the stability of feedback-controlled systems is just so important as their capacity of providing safe behaviour under a wide variety of operational circumstances. Furthermore, safety is also a mandatory property for systems with high levels of interoperability, cooperation or coordination with humans.

The notion of *safety* was first introduced in 1977 in the context of program correctness by [1] and later formalized in [2], which also introduced the concept of *liveness*. Intuitively, one can describe these two contrasting system properties as: (i) the requirement of avoiding undesired situations while (ii) guaranteeing the eventual achievement of a desired configuration, respectively. As pointed out by [3], in the context of control systems, liveness can be identified as an *asymptotic stability* requirement with respect to a certain set of desired or objective states, while safety can be defined as the *invariance* of the system trajectories to some set, defined as the set of *safe* states. While the design of asymptotically stabilizing controllers has been extensively studied in control Lyapunov theory [4], the design of controllers capable of enforcing invariance to a particular set of states has been the subject

of study in the topic of Control Barrier Functions (CBFs) [5]. Additionally, [5] also introduced the idea of unifying CBFs with Control Lyapunov Functions (CLFs) through the use of quadratic programs (QPs), effectively combining safety and stabilization requirements in a single and elegant control framework.

However, the study of controllers combining the two desirable properties of *stability* and *safety* is still in early stages. In [6], it is shown that the QP-based framework proposed by [5] can introduce undesirable equilibrium points other than the CLF minimum into the closed-loop system (see Fig. 1 that illustrates the problem). The fact that some of these undesirable equilibrium points can be asymptotically stable and are located on the *boundary* of the safe set is an important practical limitation, since the system trajectories can converge directly to a neighborhood of the unsafe set. Therefore, the QP-based framework for unifying CLFs and CBFs is able to guarantee *safety* in the form of trajectory invariance with respect to a certain (safe) set, but not *liveness* and practical *reliability*, since the closed-loop system trajectories can be attracted towards undesirable stable equilibria which are arbitrarily close to the set of unsafe states. This is an undesirable characteristic for practical applications, since it could result in system deadlocks and expose the system to close-to-failure situations, forcing the designer to opt for highly conservative safety margins when designing the system safety specifications.

In [7], an optimization-based method was proposed in which safety is ensured without introducing undesired equilibria into the closed-loop system, even in presence of multiple non-convex unsafe sets. Although representing an important step towards solving the issue of undesirable equilibria in CLF-CBF-based controllers, the method is dependent on the computation of a nonlinear “convexification” function for the unsafe sets, which can be highly dependent on the obstacle geometry and computationally hard to solve.

The present work contributes to the theory of safety-critical systems in the following ways:

- 1) We present an in-depth study of the conditions for existence and stability of equilibrium points on the closed-loop system with the minimum-norm QP-based controller proposed by [5], for the class of driftless nonlinear systems.
- 2) We derive an insightful geometric condition for determining the stability properties of boundary equilibrium points, and show that, for driftless nonlinear systems, this stability condition is independent on the system model, depending only on the geometry of the CLF and the corresponding CBF.
- 3) We introduce the property of *compatibility* between a CLF and a family of CBFs, regarding the number of

Matheus F. Reis and A. Pedro Aguiar are with the Department of Electrical and Computer Engineering from FEUP (Faculty of Engineering of University of Porto), Portugal matheus.reis@fe.up.pt, pedro.aguiar@fe.up.pt

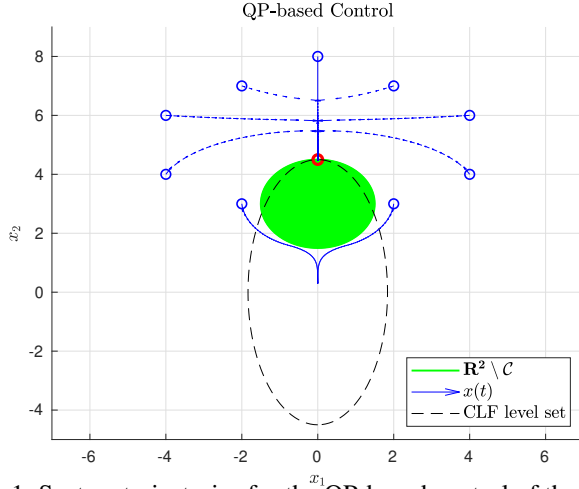


Fig. 1: System trajectories for the QP-based control of the integrator with a circular obstacle. The undesirable asymptotically stable equilibrium is shown in red.

stable equilibrium points of the closed-loop system other than the CLF minimum.

- 4) We show, for the first time, how the theory of Linear Matrix Pencils can be explored to derive sufficient compatibility conditions for the class of quadratic CLFs and CBFs.
- 5) A novel QP-based controller is proposed, aiming to adaptively modify the shape of a parametric quadratic CLF, in order to guarantee compatibility with a family of given quadratic CBFs, thus guaranteeing safety and quasi-global convergence of the closed-loop system trajectories to the CLF minimum.
- 6) Throughout the paper, we provide numerical examples aiming to illustrate the presented results and the proposed control design methodology.

II. ANALYSIS OF THE QUADRATIC PROGRAM BASED CONTROL FOR SAFETY CRITICAL SYSTEMS

In this section, we briefly present the notation used throughout this paper, followed by a detailed analysis of the closed-loop system formed by the controller proposed by [5] with a CLF and N distinct CBFs.

A. Notation

A function f is said to be of (differentiability) class C^k if its derivatives f', f'', \dots, f^k exist and are continuous. For a scalar-valued differentiable function $f: \mathbb{R}^n \rightarrow \mathbb{R}$, the operator $\nabla: C^1(\mathbb{R}^n) \rightarrow \mathbb{R}^n$ is defined as the *gradient* $\frac{\partial f}{\partial x}$, and the self-adjoint operator $H: C^2(\mathbb{R}^n) \rightarrow \mathbb{R}^{n \times n}$ is defined as the *Hessian*, with entries $(Hf)_{i,j} = \frac{\partial^2 f}{\partial x_i \partial x_j}$.

The notation $\langle u, v \rangle$ denotes the usual inner product between two vectors $u, v \in \mathbb{R}^n$, while $L_g f$ denotes the Lie derivative of f along the vector field $g: \mathbb{R}^n \rightarrow \mathbb{R}^{n \times m}$, that is, $L_g f = \nabla f^T g \in \mathbb{R}^m$, respectively. The set $\text{span}\{v_1, \dots, v_p\}$ is the linear span of a finite set of vectors $v_1, \dots, v_p \in \mathbb{R}^n$, that is, the set of all linear combinations of these vectors. The orthogonal complement of a subspace W is denoted by W^\perp .

The group of real symmetric matrices is denoted by \mathcal{S}^n , while the positive and negative semidefinite cones of the set of symmetric matrices are denoted by \mathcal{S}_+^n and \mathcal{S}_-^n , respectively. The null space and spectrum of a real square matrix $A \in \mathbb{R}^{n \times n}$ are given by $\mathcal{N}(A) \subset \mathbb{R}^n$ and $\sigma(A) \subset \mathbb{R}$, respectively. Given two arbitrary nonzero vectors $v, w \in \mathbb{R}^n$, we define $\mathcal{P}_{vw} := I_n - \frac{vw^T}{v^T w} \in \mathbb{R}^{n \times n}$, which is an oblique projection matrix defined over \mathbb{R}^n . It has the following useful properties: (i) $\mathcal{P}_{vw}^T = \mathcal{P}_{vw}$; (ii) the spectrum of \mathcal{P}_{vw} is composed of 0 and 1's with algebraic multiplicity 1 and $n-1$, respectively; (iii) $\mathcal{N}(\mathcal{P}_{vw}) = \{z \in \mathbb{R}^n \mid z = \alpha v, \forall \alpha \in \mathbb{R}\}$; (iv) $\mathcal{N}(\mathcal{P}_{vw}^T) = \{z \in \mathbb{R}^n \mid z = \alpha w, \forall \alpha \in \mathbb{R}\}$; (v) $\mathcal{P}_{vw} z = z$ for all $z \in \mathbb{R}^n$ s.t. $z^T w = 0$; (vi) $z^T \mathcal{P}_{vw} = z^T$ for all $z \in \mathbb{R}^n$ s.t. $z^T v = 0$. Additionally, we define $\mathcal{P}_{vv} = \mathcal{P}_v = I_n - \hat{v}\hat{v}^T$ as the orthogonal projection matrix defined over \mathbb{R}^n .

The set $\mathcal{SO}(n)$ is the special orthogonal group of dimension n , consisting of all orthogonal matrices R , i.e., $R^T R = I_n$ of determinant 1, and the set $\mathfrak{so}(n)$ consists of the corresponding Lie algebra of $\mathcal{SO}(n)$. Lastly, the cardinality of a set \mathcal{S} is the number of elements on \mathcal{S} , and is denoted by $|\mathcal{S}|$.

B. QP-based Controller with Multiple CBFs

Consider now the *driftless, affine* nonlinear control system

$$\dot{x} = g(x)u \quad (1)$$

where $x \in \mathbb{R}^n$ is the system state and $u \in \mathbb{R}^m$ is the control input. The vector field $g: \mathbb{R}^n \rightarrow \mathbb{R}^{n \times m}$ is locally Lipschitz. In particular, $g(x)$ is full rank for all values of $x \in \mathbb{R}^n$.

Definition II.1 (CLFs). A *positive definite function* V is a *control Lyapunov function (CLF)* for system (1) if it satisfies:

$$\inf_{u \in \mathbb{R}^m} [\langle L_g V(x), u \rangle] \leq -\gamma(V(x))$$

where $\gamma: \mathbb{R}_{\geq 0} \rightarrow \mathbb{R}_{\geq 0}$ is a class \mathcal{K} function [8].

For a given V , this definition implies that there exists a set of stabilizing controls that makes the CLF strictly decreasing everywhere outside its global minimum $x_0 \in \mathbb{R}^n$. This set is defined by

$$\mathcal{K}_{clf}(x) = \{u \in \mathbb{R}^m : \langle L_g V(x), u \rangle \leq -\gamma(V(x))\}.$$

Let $u^*(x)$ be a feedback controller such that the closed-loop system

$$\dot{x} = f_{cl}(x) := g(x)u^*(x) \quad (2)$$

is locally Lipschitz. Then, for any initial condition $x(0) \in \mathbb{R}^n$ there exists a maximum interval of existence $I(x(0)) = [0, \tau_{max})$ such that $x(t)$ is the unique solution to (2) on $I(x(0))$ (if $f_{cl}(x)$ is forward complete, $\tau_{max} = \infty$). A set \mathcal{C} is *forward invariant* if, for every $x(0) \in \mathcal{C}$, $x(t) \in \mathcal{C}$ for all $t \in I(x(0))$.

Definition II.2 (Safety). The *trajectories of the closed-loop system (2) are safe with respect to a set \mathcal{C} if \mathcal{C} is forward invariant*.

Then, consider N subsets $\mathcal{C}_1, \dots, \mathcal{C}_N \subset \mathbb{R}^n$ defined by the superlevel set of a continuously differentiable function $h_i: \mathbb{R}^n \rightarrow \mathbb{R}$:

$$\mathcal{C}_i = \{x \in \mathbb{R}^n : h_i(x) \geq 0\} \quad (3)$$

Definition II.3 (CBFs). Let $\mathcal{C}_i \in \mathbb{R}^n$ be defined by one of the functions (3). Then $h_i(x)$ is a (zeroing) Control Barrier Function (CBF) for (1) if there exists a locally Lipschitz extended class \mathcal{K}_∞ function¹ α such that

$$\sup_{u \in \mathbb{R}^m} [\langle L_g h_i(x), u \rangle] \geq -\alpha(h_i(x)) \quad \forall x \in \mathbb{R}^n.$$

The definition simply means that the CBFs $h_i(x)$ are only allowed to decrease in the interior of their respective safe sets $\text{int}(\mathcal{C}_i)$, but not on their boundaries $\partial\mathcal{C}_i$. Then, the set of control values that render the safe set $\mathcal{C} = \cap_{i=1}^N \mathcal{C}_i$ forward invariant can be defined as:

$$\begin{aligned} \mathcal{K}_{cbf}(x) &= \cap_{i=1}^N \mathcal{K}_{cbf_i}(x), \\ \mathcal{K}_{cbf_i}(x) &= \{u \in \mathbb{R}^m : \langle L_g h_i(x), u \rangle + \alpha h_i(x) \geq 0\}. \end{aligned} \quad (4)$$

A proposed minimum-norm controller based on [5] with N CBFs is given by

$$\begin{aligned} \min_{(u, \delta) \in \mathbb{R}^{m+1}} & \frac{1}{2} \|u\|^2 + \frac{1}{2} p \delta^2 & (5) \\ \text{s.t.} & \langle L_g V(x), u \rangle + \gamma V(x) \leq \delta & \text{(CLF)} \\ & \langle L_g h_1(x), u \rangle + \alpha h_1(x) \geq 0 & \text{(1st CBF)} \\ & \vdots \\ & \langle L_g h_N(x), u \rangle + \alpha h_N(x) \geq 0 & \text{(N-th CBF)} \end{aligned}$$

where $p, \gamma, \alpha > 0$. The objective is to minimize the norm of the control signal and of an auxiliary *relaxation* variable δ while satisfying the CLF and CBF constraints. The CBF constraints guarantee that $u \in \mathcal{K}_{cbf}(x)$, keeping the system trajectories safe with respect to the safe set $\mathcal{C} = \cap_{i=1}^N \mathcal{C}_i$.

Assumption II.1. The initial state $x(0) \in \mathbb{R}^n$ is contained in the safe set, that is, $x(0) \in \mathcal{C} = \cap_{i=1}^N \mathcal{C}_i$.

Theorem 1. The QP (5) is feasible under Assumption II.1.

Proof. Under Assumption II.1, $h_i(x(0)) \geq 0$ for all $i = 1, \dots, N$. Then, all the half-planes defined by $\mathcal{K}_{cbf_i}(x(0)) \subset \mathbb{R}^m$ in (4) contain the origin $u = 0$ (due to the fact that $h_i(x(0)) \geq 0$). Then, their intersection $\cap_{i=1}^N \mathcal{K}_{cbf_i}(x(0))$ is always non-empty and forms a convex polytope in \mathbb{R}^m containing the origin $u = 0$.

In the QP decision space \mathbb{R}^{m+1} , due to the independence of the CBF constraints on δ , they form an unbounded convex polytope in \mathbb{R}^{m+1} containing the δ -axis: that is, every point on the QP decision space of the form $(u, \delta) = (0, d) \forall d \in \mathbb{R}$ is contained within $\cap_{i=1}^N \mathcal{K}_{cbf_i}(x(0)) \times \mathbb{R}$. Since the CLF constraint defines a half-space in \mathbb{R}^{m+1} that always intersects this unbounded polytope, we conclude that the QP (5) is initially feasible under Assumption II.1, since the feasible region is always non-empty.

Since the CBF constraints guarantee the invariance of $x(t)$ with respect to the safe set $\mathcal{C} = \cap_{i=1}^N \mathcal{C}_i$, the same reasoning can be applied for any time $t \geq 0$, and we can conclude that the QP (5) is always feasible under Assumption II.1. \square

¹An extended class \mathcal{K}_∞ function $\alpha : \mathbb{R} \rightarrow \mathbb{R}$ is strictly increasing with $\alpha(0) = 0$.

C. Existence of Equilibrium Points

We now extend an important result from [6], regarding the existence of equilibrium points in the case with multiple CBF constraints. Particularly, Theorem 2 shows that the driftless, affine closed-loop system with the QP-based controller can have undesirable equilibrium points other than the CLF global minimum, and all of them are located on the boundaries of the safe sets. In this work, for generality purposes, we assume the CLF global minimum to be located at an arbitrary point $x_0 \in \mathbb{R}^n$ such that $V(x_0) = 0$.

Assumption II.2. The CLF global minimum $x_0 \in \mathbb{R}^n$ is contained in the safe set: $x_0 \in \mathcal{C} = \cap_{i=1}^N \mathcal{C}_i \subset \mathbb{R}^n$. Furthermore, the boundaries of the safe sets are disjoint, that is, $\partial\mathcal{C}_i \cap \partial\mathcal{C}_j = \emptyset \forall i \neq j, i = 1, \dots, N$.

Notice that the first part of Assumption II.2 is naturally required, since it is impossible to achieve asymptotic stability of the CLF minimum with controller (5) if $x_0 \notin \mathcal{C}$, since in that case the CLF minimum x_0 would be contained in the unreachable unsafe set. The second part of the assumption is reasonable for obstacle-scattered environments, where each CBF models one particular convex obstacle.

Theorem 2. Under Assumption II.2, the set \mathcal{E} of equilibrium points of the closed-loop system resulting from the application of the control law (5) into (2) is given by

$$\begin{aligned} \mathcal{E} &= (\cup_{i=1}^N \mathcal{E}_i) \cup \{x_0\}, & i = 1, \dots, N & (6) \\ \mathcal{E}_i &= \left\{ x \in \partial\mathcal{C}_i \mid \nabla V = \lambda_i \nabla h_i, \lambda_i = \frac{\langle L_g V, L_g h_i \rangle}{\langle L_g h_i, L_g h_i \rangle} > 0 \right\} \end{aligned}$$

In particular, (6) implies that equilibria other than x_0 are located on the boundaries $\partial\mathcal{C}_1, \dots, \partial\mathcal{C}_N$.

Proof. Define the Lagrange multipliers of the optimization problem (5) as $\lambda_0, \bar{\lambda}_1, \dots, \bar{\lambda}_N$, where λ_0 refers to the multiplier of the CLF constraint and $\bar{\lambda}_i$ refers to the multiplier of the i -th CBF constraint. Let $\lambda_i = \bar{\lambda}_i / \lambda_0$ be a normalized version of the Lagrange multiplier $\bar{\lambda}_i$, defined when the CLF constraint is active, that is, $\lambda_0 > 0$. The Lagrangian associated to QP (5) is given by

$$\begin{aligned} \mathcal{L} &= \frac{1}{2} \|u\|^2 + \frac{1}{2} p \delta^2 + \lambda_0 (\langle L_g V, u \rangle + \gamma V - \delta) & (7) \\ & - \sum_{j=1}^N \bar{\lambda}_j (\langle L_g h_j, u \rangle + \alpha h_j) \end{aligned}$$

The KKT (Karush-Kuhn-Tucker) optimality conditions yield the following conditions

$$\frac{\partial \mathcal{L}}{\partial u} = u + \lambda_0 L_g V - \lambda_0 \sum_{j=1}^N \lambda_j L_g h_j = 0 \quad (8)$$

$$\frac{\partial \mathcal{L}}{\partial \delta} = p \delta - \lambda_0 = 0 \quad (9)$$

$$\lambda_0 (\langle L_g V, u \rangle + \gamma V - \delta) = 0 \quad (10)$$

$$\bar{\lambda}_j (\langle L_g h_j, u \rangle + \alpha h_j) = 0 \quad (11)$$

with $j = 1, \dots, N$ in (11), and $\lambda_j \geq 0$. Equation (8) yields an analytical expression for the feedback controller

$$u^*(x) = \lambda_0 \left(-L_g V + \sum_{j=1}^N \lambda_j L_g h_j \right) \quad (12)$$

Equation (9) yields $\lambda_0 = p\delta$. Next, assume that the CLF constraint is inactive at some region: in this case, $\dot{V} + \gamma V = \langle \nabla V, f_{cl} \rangle + \gamma V < \delta$ and using (10), $\lambda_0 = 0$, implying that $\delta = 0$. Since $f_{cl}(x^*) = 0$ at an equilibrium point x^* , we conclude that $\gamma V < 0$, which is a contradiction since $V(x)$ is a positive definite function. Therefore, we conclude that equilibrium points can only occur when the CLF constraint is active.

Therefore, at an equilibrium point x^* , the following equation always holds

$$\underbrace{\langle \nabla V(x^*), f_{cl}(x^*) \rangle}_{=0} + \gamma V(x^*) = \delta$$

Then, $\lambda_0^* = p\delta = p\gamma V(x^*)$ at the equilibrium point. Notice that the global minimum of the CLF $x_0 \in \mathcal{C}$ is a trivial equilibrium solution, since $h_i(x_0) \geq 0$ and $V(x_0) = 0$, with $\delta = 0$.

Now, assume that the i -th CBF constraint is active. In this case, we have $\dot{h}_i + \alpha h_i = 0$. At an equilibrium point x^* , we have $\dot{h}_i = \langle \nabla h_i(x^*), f_{cl}(x^*) \rangle = \langle \nabla h_i(x^*), 0 \rangle = 0$, implying that $h_i(x^*) = 0$. This shows that $x^* \in \partial \mathcal{C}_i$.

Next, we show that, under Assumption II.2, these equilibrium points can only occur when *one and only one* of the CBF constraints are active. Assume that an equilibrium point x^* occurs when two or more CBF constraints are active: then, we have $\dot{h}_i + \alpha h_i(x^*) = 0$ and $\dot{h}_j + \alpha h_j(x^*) = 0$, for $i \neq j$. In equilibrium, $\dot{h}_i = \langle L_g h_i(x^*), u \rangle = 0$ and $\dot{h}_j = \langle L_g h_j(x^*), u \rangle = 0$, which means that $h_i(x^*) = h_j(x^*) = 0$. However, by the second part of Assumption II.2, this is a contradiction since $\partial \mathcal{C}_i \cap \partial \mathcal{C}_j = \emptyset$, and therefore $x^* \notin \partial \mathcal{C}_i \cap \partial \mathcal{C}_j$. The conclusion is that boundary equilibrium points can only occur when *one and only one* of the CBF constraints are active.

Combining (12) with the closed-loop system (2) yields

$$\dot{x} = f_{cl}(x) = \lambda_0 G(x) \left(-\nabla V + \sum_{j=1}^N \lambda_j \nabla h_j \right) \quad (13)$$

where $G(x) = g(x)g(x)^\top$. Notice that since $G(x)$ is full rank by assumption. Therefore, using (13), at an equilibrium point, the following condition must be satisfied:

$$\nabla V(x^*) = \sum_{j=1}^N \lambda_j \nabla h_j(x^*). \quad (14)$$

In (14), assume that the equilibrium point $x^* \in \partial \mathcal{C}_i$ is located at the i -th boundary. Since the only active constraints are the CLF and the i -th CBF constraint, we have $\lambda_j = 0, \forall j \neq i$, simplifying the equilibrium condition (14) to $\nabla V(x^*) = \lambda_i \nabla h_i(x^*)$. Furthermore, the control expression (12) simplifies to $u(x^*) = \lambda_0^* g^\top (-\nabla V + \lambda_i \nabla h_i)$. Replacing

$u(x^*)$ on the expression for the i -th active CBF constraint yields

$$-\lambda_0^* \langle L_g V, L_g h_i \rangle + \lambda_0^* \lambda_i \langle L_g h_i, L_g h_i \rangle = \alpha h_i(x^*) = 0 \quad (15)$$

Dividing (15) by $\lambda_0^* > 0$, we conclude that

$$\lambda_i = \frac{\langle L_g V, L_g h_i \rangle}{\langle L_g h_i, L_g h_i \rangle},$$

which formally justifies the definition of set $\mathcal{E}_i \subset \partial \mathcal{C}_i$. \square

D. Stability of Equilibrium Points

In this section, we study the stability properties for the boundary equilibrium points from Theorem 2. We start with the following result.

Lemma 1. *The Jacobian matrix of the closed-loop system (2) with u^* from (5) at an equilibrium point $x^* \in \mathcal{E}_i$ is given by*

$$J_{cl}(x^*) = \lambda_0^* \mathcal{P}_i G H_i - \frac{\alpha}{\|\nabla h_i\|_G^2} G \nabla h_i \nabla h_i^\top, \quad (16)$$

where $\mathcal{P}_i = \mathcal{P}_{G \nabla h_i \nabla h_i}$ is an oblique projection matrix and $H_i = \lambda_i^* H_{h_i, i} - H_V$, with

$$\lambda_0^* = p\gamma V(x^*), \quad \lambda_i^* = \frac{\langle L_g V(x^*), L_g h_i(x^*) \rangle}{\langle L_g h_i(x^*), L_g h_i(x^*) \rangle}.$$

Furthermore, H_V and $H_{h_i, i}$ are the Hessian matrices of V and h_i , respectively.

Proof. Taking the partial derivative of the closed-loop system (13) with respect to the k -th state variable yields:

$$\begin{aligned} \frac{\partial f_{cl}}{\partial x_k} &= \frac{\partial(\lambda_0 G(x))}{\partial x_k} \left(-\nabla V + \sum_{j=1}^N \lambda_j \nabla h_j \right) \\ &+ \lambda_0 G(x) \left(\sum_{j=1}^N \left(\lambda_j \frac{\partial \nabla h_j}{\partial x_k} + \frac{\partial \lambda_j}{\partial x_k} \nabla h_j \right) - \frac{\partial \nabla V}{\partial x_k} \right) \end{aligned} \quad (17)$$

From the equilibrium conditions valid on $x^* \in \mathcal{E}_i$, the first term in parenthesis vanishes. Furthermore, on the second sum on (17), we know that $\lambda_j = 0, \forall j \neq i$. Then, define the open set of points where only the i -th CBF constraint is active as

$$\mathcal{S}_i = \{x \in \mathbb{R}^n \mid \langle L_g h_i(x), u^*(x) \rangle + \alpha h_i(x) = 0, \langle L_g h_j(x), u^*(x) \rangle + \alpha h_j(x) > 0, \forall j \neq i\}, \quad (18)$$

where $u^*(x)$ is given by the QP solution (12). Notice that $\lambda_i(x) > 0$ and $\lambda_j(x) = 0 (j \neq i)$ for all $x \in \mathcal{S}_i$. Therefore, \mathcal{S}_i contains the equilibrium point $x^* \in \mathcal{E}_i$, since only the i -th CBF constraint is active (that is, $\lambda_i(x^*) > 0, \lambda_j(x^*) = 0, \forall j \neq i$). Therefore, on $x^* \in \mathcal{E}_i$, $\frac{\partial \lambda_j}{\partial x_k} = 0, \forall j \neq i$ on the second sum of (17). Then, (17) reduces to

$$\begin{aligned} \frac{\partial f_{cl}}{\partial x_k} &= \lambda_0^* G(x^*) \left([H_i]_k + \frac{\partial \lambda_i}{\partial x_k} \nabla h_i \right), \\ [H_i]_k &= \lambda_i \frac{\partial \nabla h_i}{\partial x_k} - \frac{\partial \nabla V}{\partial x_k} \end{aligned} \quad (19)$$

Notice that (19) is the k -th column of the Jacobian matrix at the equilibrium point. Besides, this expression shows that on $x^* \in \mathcal{E}_i$, the Jacobian $J_{cl}(x^*)$ is not dependent on the other

CBFs $h_j(x)$, $j \neq i$. Similarly, the partial derivatives of ∇h_i and ∇V with respect to x_k are the columns of the Hessian matrices of h_i and V , respectively. Then, $[H_i]_k$ is the k -th column of matrix $H_i = \lambda_i^* H_{h,i} - H_V$.

Next, taking the partial derivative of (15) with respect to x_k and applying the equilibrium condition $\nabla V = \lambda_i \nabla h_i$ yields

$$\frac{\partial \lambda_i}{\partial x_k} = -\frac{1}{\lambda_0^* \|\nabla h_i\|^2} \left(\lambda_0^* \nabla h_i^\top G [H_i]_k - \alpha \frac{\partial h_i}{\partial x_k} \right) \quad (20)$$

Substituting (20) into (19) yields:

$$\frac{\partial f_{cl}^*}{\partial x_k} = \lambda_0^* \mathcal{P}_{G\nabla h_i, \nabla h_i} G [H_i]_k - \frac{\alpha}{\|\nabla h_i\|_G^2} [\nabla h_i]_k G \nabla h_i$$

where $[\nabla h_i]_k$ denotes the k -th component of ∇h_i . The expression above is simply the k -th column of (16), thus concluding the demonstration. \square

In [6, Theorem 2], it was shown that some of these boundary equilibria can be asymptotically stable even for a simple integrator system. Here, we generalize that result for the driftless nonlinear closed-loop system (2) with control $u^*(x)$ from (5). Specifically, we derive a necessary and sufficient condition under which the boundary equilibria is *unstable*.

Theorem 3. *Consider the system (1) with $u = u^*(x)$ given by (5), and assume that the CLF minimum $x_0 \in \text{int}(\mathcal{C})$. A boundary equilibrium point $x^* \in \mathcal{E}_i$ is unstable if and only if there exists a direction $z \in \text{span}\{\nabla V(x^*)\}^\perp \equiv \text{span}\{\nabla h_i(x^*)\}^\perp$ such that*

$$\lambda_i^* \mathcal{D}_z^2 h_i(x^*) - \mathcal{D}_z^2 V(x^*) > 0, \quad (21)$$

where $\mathcal{D}_z^2 V(x^*) = z^\top H_V z$ and $\mathcal{D}_z^2 h_i(x^*) = z^\top H_{h,i} z$ are the second directional derivatives of V and h_i evaluated at $x^* \in \mathcal{E}_i$, respectively.

Proof. Using the expression for the Jacobian matrix in the equilibrium point (16) and computing the inner product between the eigenvalue equation $J_{cl}(x^*)v_k = \sigma_k v_k$ and $\nabla h_i(x^*)$ yields

$$\nabla h_i^\top J_{cl}(x^*) v_k = -\alpha \nabla h_i^\top v_k = \sigma_k \nabla h_i^\top v_k,$$

where the property (iv) of the oblique projection matrix was used. The equation above shows that the eigenvalues associated to eigenvectors that are not perpendicular to ∇h_i are $\sigma_k = -\alpha < 0$, due to the fact that $\alpha > 0$. Then, the corresponding eigenvalue equation $J_{cl}(x^*)v_k = -\alpha v_k$ can be rewritten as

$$\mathcal{P}_i (\lambda_0^* G H_i + \alpha I_n) v_k = 0 \quad (22)$$

From (22), two conclusions can be drawn:

- 1) $(-\alpha, v_k)$ is an eigenpair of $\lambda_0^* G H_i$: if $-\alpha$ is an eigenvalue of $\lambda_0^* G H_i$ with geometric multiplicity s , then the corresponding eigenvectors v_k of $\lambda_0^* G H_i$ associated to $-\alpha$ satisfy (22), and are also eigenvectors of $J_{cl}(x^*)$, with associated eigenvalue $-\alpha$.
- 2) $-\alpha$ is not an eigenvalue of $\lambda_0^* G H_i$: in this case, $\lambda_0^* G H_i + \alpha I_n$ is nonsingular. By property (iii) of the oblique projection matrix, the null space of $\mathcal{P}_{G\nabla h_i, \nabla h_i}$

is a one dimensional subspace generated by $G\nabla h_i$. Therefore, the unique solution for (22) is

$$v_k = \beta (\lambda_0^* G H_i + \alpha I_n)^{-1} G \nabla h_i, \quad \beta \in \mathbb{R},$$

describing the corresponding (unique) eigenvector associated to eigenvalue $-\alpha$.

From the above, we conclude the following: $J_{cl}(x^*)$ has between 1 and s stable eigenvalues equal to $-\alpha$, with corresponding eigenvectors satisfying $\nabla h_i^\top v_k \neq 0$. In this case, all the remaining $n - s$ to $n - 1$ eigenvalues of $J_{cl}(x^*)$ must be associated to corresponding eigenvectors $v_k \in \mathbb{R}^n$ lying on the orthogonal complement of $\nabla h_i(x^*)$, that is, $\nabla h_i(x^*)^\top v_k = 0$. Therefore, the stability of $x^* \in \mathcal{E}_i$ is fully characterized by the eigenpairs $(\sigma_k, v_k) \in \mathbb{R} \times \mathbb{R}^n$ such that $v_k \in \text{span}\{\nabla h_i(x^*)\}^\perp$.

Using (16), the corresponding eigenvalue equation for these eigenpairs is given by $J_{cl}(x^*)v_k = G_i H_i v_k = \sigma_k v_k$, where $G_i = \mathcal{P}_i G$. This eigenvalue equation can also be rewritten as

$$G_i H_i v_k = \sigma_k v_k \quad (23)$$

Therefore, we can use (23) to draw conclusions on the stability properties of $x^* \in \mathcal{E}_i$. This can be done by analysing the spectrum of $G_i H_i$: since $G_i = G_i^\top \geq 0$, it can be written as $G_i = G_i^{\frac{1}{2}} G_i^{\frac{1}{2}}$, where $G_i^{\frac{1}{2}}$ is the symmetric positive semidefinite square root of G_i . Define matrix $G_i^{\frac{1}{2}} H_i G_i^{\frac{1}{2}}$, which has the following eigenvalue equation:

$$G_i^{\frac{1}{2}} H_i G_i^{\frac{1}{2}} w_k = \sigma_k^* w_k, \quad (24)$$

where $(\sigma_k^*, w_k) \in \mathbb{R} \times \mathbb{R}^n$ are eigenpairs of $G_i^{\frac{1}{2}} H_i G_i^{\frac{1}{2}}$. Since $G_i^{\frac{1}{2}} H_i G_i^{\frac{1}{2}}$ is symmetric, its n eigenvectors form an orthonormal basis for \mathbb{R}^n , i.e. $w_k^\top w_j = \delta_{kj}$ (δ_{kj} is the Kronecker delta). Left-multiplying both sides of (24) by $G_i^{\frac{1}{2}}$ yields

$$G_i^{\frac{1}{2}} G_i^{\frac{1}{2}} H_i G_i^{\frac{1}{2}} w_k = G_i H_i \underbrace{G_i^{\frac{1}{2}} w_k}_{v_k} = \sigma_k^* \underbrace{G_i^{\frac{1}{2}} w_k}_{v_k} \quad (25)$$

Note that (25) and (23) are the same eigenvalue equation for $\sigma_k^* \neq 0$, revealing that $G_i H_i$ and $G_i^{\frac{1}{2}} H_i G_i^{\frac{1}{2}}$ share the same nonzero eigenvalues ($\sigma_k = \sigma_k^* \neq 0$). Furthermore, the corresponding eigenvectors of $G_i H_i$ are given by $v_k = G_i^{\frac{1}{2}} w_k$. Then, left-multiplying (24) by w_j^\top yields

$$w_j^\top H_i v_k = \sigma_k \delta_{kj} \quad (26)$$

One can now conclude the following. Consider first that $x^* \in \mathcal{E}_i$ is unstable. Then, some of the eigenvalues of $G_i H_i$ must be strictly positive, that is, $\exists \sigma_k > 0$ for some k . Using (26):

$$\begin{aligned} \sigma_k &= v_k^\top H_i v_k = \lambda_i^* v_k^\top H_{h,i} v_k - v_k^\top H_V v_k \\ &= \lambda_i^* \mathcal{D}_{v_k}^2 h_i(x^*) - \mathcal{D}_{v_k}^2 V(x^*) > 0 \end{aligned}$$

which shows that $z = v_k \in \text{span}\{\nabla h_i(x^*)\}^\perp$ represents a direction s.t. condition (21) is true. Thus, sufficiency of the condition in Theorem 3 is proven.

Now consider that $\exists z \in \text{span}\{\nabla h_i(x^*)\}^\perp$ s.t. (21) is true. Note that condition (21) is equivalent to $z^\top H_i z > 0$. Since $z \in \text{span}\{\nabla h_i(x^*)\}^\perp$, it can be expanded in terms of the

eigenvectors of $G_i H_i$, as $z = \sum_{k=1}^n \beta_k v_k$, where $\beta_k \in \mathbb{R}$. Using this expansion and (26), $z^\top H_i z$ yields

$$z^\top H_i z = \sum_{k,j} \beta_k \beta_j v_k^\top H_i v_j = \sum_k \beta_k^2 \sigma_k > 0,$$

which means that there exists at least one $\sigma_k > 0$. Then, $x^* \in \mathcal{E}_i$ is unstable. Thus, necessity of the condition in Theorem 3 is proven. \square

Remark II.1. *Theorem 3 has the following geometric meaning. At any equilibrium point $x^* \in \mathcal{E}_i$, the orthogonal complements $\text{span}\{\nabla V(x^*)\}^\perp$ and $\text{span}\{\nabla h_i(x^*)\}^\perp$ are equivalent vector spaces. Thus, one can define the sectional curvatures of V and h_i at some direction $z \in \text{span}\{\nabla V(x^*)\}^\perp \equiv \text{span}\{\nabla h_i(x^*)\}^\perp$ as*

$$\begin{aligned} \kappa_v(x^*, z) &= \frac{1}{\|\nabla V\|} \langle \hat{z}, H_V \hat{z} \rangle, \\ \kappa_{h,i}(x^*, z) &= \frac{1}{\|\nabla h_i\|} \langle \hat{z}, H_{h,i} \hat{z} \rangle. \end{aligned}$$

Then, condition (21) can be precisely rewritten as a difference of sectional curvatures at the orthogonal complements, that is,

$$\begin{aligned} \Delta \kappa_i(x^*, z) &= \kappa_{h,i}(x^*, z) - \kappa_v(x^*, z) \\ &= \frac{1}{\|\nabla h_i\|} \langle \hat{z}, H_{h,i} \hat{z} \rangle - \frac{1}{\|\nabla V\|} \langle \hat{z}, H_V \hat{z} \rangle \\ &= \frac{1}{|\lambda_i^*| \|\nabla h_i\| \|z\|^2} (|\lambda_i^*| \mathcal{D}_z^2 h_i - \mathcal{D}_z^2 V) > 0 \end{aligned} \quad (27)$$

Therefore, since $\lambda_i^* > 0$, conditions (21) and (27) are equivalent: if there exists a direction $\hat{z} \in \text{span}\{\nabla V(x^*)\}^\perp \equiv \text{span}\{\nabla h_i(x^*)\}^\perp$ such that the sectional curvature of V is smaller than the sectional curvature of h_i , then $x^* \in \mathcal{E}_i$ is unstable. The reason lies in geometry: \hat{z} represents a direction under which the trajectories of the closed-loop system (2) under control (5) cause the CLF V to decrease, while still remaining inside of the safe set \mathcal{C}_i .

In light of Theorem 3, we now define the concept of compatibility between a CLF and a family of CBFs.

Definition II.4 (Compatibility). *The CLF V is compatible with the family of CBFs $\{h_1, h_2, \dots, h_N\}$ if the CLF global minimum $x_0 \in \mathbb{R}^n$ is the only stable equilibrium point of the closed-loop system (2) with controller (5).*

Corollary 1. *The CLF V is compatible with the family of CBFs $\{h_1, h_2, \dots, h_N\}$ if and only if:*

- (i) $x_0 \in \mathcal{C} = \cap_{i=1}^N \mathcal{C}_i$
- (ii) $\forall x^* \in \mathcal{E}_i$, there always exists a direction $z \in \mathcal{T}_{x^*} V \equiv \mathcal{T}_{x^*} h_i$ such that $\Delta \kappa_i(x^*, z) > 0$, $i = 1, \dots, N$.

Proof. Theorem 2 shows that the set of equilibrium points of the closed-loop system (2) with controller (5) is given by $(\cup_{i=1}^N \mathcal{E}_i) \cup \{x_0\}$. Therefore, if condition $\Delta \kappa_i(x^*, z) > 0$ holds for some $z \in \mathcal{T}_{x^*} V \equiv \mathcal{T}_{x^*} h_i$ and for every equilibrium point $x^* \in \mathcal{E}_i$, then the set of stable equilibria of (2) reduce to $\{x_0\}$, since equilibria in $\cup_{i=1}^N \mathcal{E}_i$ are all guaranteed to be unstable. \square

III. ANALYSIS FOR QUADRATIC CLF-CBF PAIRS

Due to the geometric complexity that can be involved in the level set of general pairs of multivariate functions, it can be very difficult to guarantee compatibility for general CLF-CBF pairs. For the case that the CLF-CBF pair is a general \mathcal{C}^2 function, the quadratic approximation is the simplest function that encodes information about the local curvature of the level sets, which according to Theorem 3 is paramount to determine stability of the resulting closed-loop equilibrium points.

In this section, we present key results regarding the analytical solutions for the boundary equilibria in (6) and present sufficient conditions for compatibility, in the case of quadratic CLF-CBF pairs. To this end, we first present a brief introduction to Matrix Pencil Theory, which is of central importance on the theoretical developments that follow thereafter.

A. Matrix Pencil Theory

A real symmetric linear matrix pencil is a matrix-valued operator $P: \mathbb{R} \rightarrow \mathcal{S}^n$, where $P(\lambda) = \lambda A - B$, with $A, B \in \mathcal{S}^n$ [9]. The solutions of the *generalized eigenvalue problem*

$$P(\lambda_i) z_i = 0, \quad i = 1, \dots, n \quad (28)$$

are the n eigenpairs (λ_i, z_i) , composed of n eigenvalues $\lambda_i \in \mathbb{C}$ and n eigenvectors $z_i \in \mathbb{R}^n$ of the real, symmetric matrix pencil $P(\lambda)$. These pencil eigenvalues define the pencil *spectrum* $S_P = \{\lambda \in \mathbb{C} : \det(P(\lambda)) = 0\} \subset \mathbb{C}$. In general, pencil eigenvalues are complex numbers. However, if either A or B are definite matrices, then $S_P \subset \mathbb{R}$ (see [10]).

Definition III.1. *Let $P(\lambda) = \lambda A - B$ be a real symmetric matrix pencil with A invertible and real spectrum S_P . An eigenvalue of $P(\lambda)$ of positive type is an eigenvalue λ_i such that $z_i^\top A z_i > 0$ for the corresponding eigenvector z_i . Similarly, an eigenvalue of $P(\lambda)$ of negative type is an eigenvalue λ_i such that $z_i^\top A z_i < 0$ for the corresponding eigenvector z_i . The sets of eigenvalues of $P(\lambda)$ of positive and negative type are denoted by S_P^+ and S_P^- , respectively. Moreover, $S_P = S_P^+ \cup S_P^-$.*

Remark III.1. *By definition, if $A > 0$, $S_P = S_P^+$, $S_P^- = \emptyset$ (all pencil eigenvalues of positive type). Similarly, if $A < 0$, $S_P = S_P^-$, $S_P^+ = \emptyset$ (all pencil eigenvalues of negative type).*

Lemma 2 (Matrix Pencil Diagonalization). *Let $P(\lambda) = \lambda A - B \in \mathcal{S}^n$ be a real symmetric matrix pencil with an invertible matrix A and real spectrum S_P . Then, the matrix $Z = [z_1 \ \dots \ z_n] \in \mathbb{R}^{n \times n}$ is nonsingular and*

$$Z^\top A Z = \begin{bmatrix} I_p & 0 \\ 0 & -I_{n-p} \end{bmatrix}, \quad Z^\top B Z = \begin{bmatrix} \Lambda_P^+ & 0 \\ 0 & -\Lambda_P^- \end{bmatrix}, \quad (29)$$

where $\Lambda_P^+ = \text{diag}\{\lambda_1, \dots, \lambda_p\}$, $\Lambda_P^- = \text{diag}\{\lambda_{p+1}, \dots, \lambda_n\}$ are diagonal matrices with the p pencil eigenvalues of positive type and the $n - p$ eigenvalues of negative type, respectively. The columns of Z are the pencil eigenvectors of $P(\lambda)$.

Proof. See [9, Lemma 1.1]. \square

Lemma 3. *Let $P(\lambda) = \lambda A - B \in \mathcal{S}^n$ be a real symmetric matrix pencil with an invertible matrix A and real spectrum S_P .*

1) If $A > 0$, then:

$$P(\lambda) > 0, \quad \forall \lambda > \max S_P, \quad (30)$$

$$P(\lambda) < 0, \quad \forall \lambda < \min S_P. \quad (31)$$

2) If A is indefinite, but the pencil eigenvalues of positive and negative type are separated, then there exists an interval where $P(\lambda)$ is definite. In particular, if $\max S_P^+ < \min S_P^-$, $P(\lambda) > 0$ in the open interval $\lambda \in (\max S_P^+, \min S_P^-)$.

Proof. The proof of this interesting and important result in Matrix Pencil Theory can be found in [9, Theorem 1.2]. \square

B. Equilibrium Solutions with Quadratic CLF-CBFs

Consider that the CLF and the family of CBFs are given by the following irreducible quadratic polynomials on \mathbb{R}^n , respectively:

$$2V(x, \Pi_V) = \Delta x_0^\top H_V \Delta x_0 \geq 0, \quad \Delta x_0 = x - x_0 \quad (32)$$

$$2h(x, \Pi_{h,i}) = \Delta x_i^\top H_{h,i} \Delta x_i - 1, \quad \Delta x_i = x - x_i \quad (33)$$

where $\Pi_V = \{x_0, H_V\}$, $\Pi_{h,i} = \{x_i, H_{h,i}\}$ are parameters: the critical points $x_i \in \mathbb{R}^n$, $i = 0, 1, \dots, N$ and the symmetric, positive definite Hessian matrices $H_V, H_{h,i} \in \mathcal{S}^n$, $i = 1, \dots, N$. Notice that the level sets of irreducible quadratic polynomials with positive definite Hessians are n -dimensional ellipses. From (33), the boundary set $\partial\mathcal{C}_i$ is defined by

$$\partial\mathcal{C}_i = \{x \in \mathbb{R}^n \mid \Delta x_i^\top H_{h,i} \Delta x_i = 1\}. \quad (34)$$

From Theorem 2, substituting the gradients of (32)-(33) into the equation $\nabla V = \lambda \nabla h_i$ with the transformation $v_i = \Delta x_i$ and using (34), the equilibrium solutions are given by the following system of $n + 1$ nonlinear equations in $n + 1$ variables:

$$H_i(\lambda)v_i = w_i, \quad \lambda_i > 0 \quad (35)$$

$$v_i^\top H_{h,i} v_i = 1, \quad (36)$$

where $H_i = \lambda H_{h,i} - H_V$ is a real symmetric matrix pencil on variable λ and $w_i = H_V(x_i - x_0) \in \mathbb{R}^n$. For $\lambda \notin S_{H_i}$, the pencil $H_i(\lambda)$ is invertible and (35) can be immediately solved, yielding $v_i(\lambda) = H_i(\lambda)^{-1}w_i$. In this case, one can define the following scalar function:

$$\begin{aligned} q_i(\lambda) &= v_i(\lambda)^\top H_{h,i} v_i(\lambda) \\ &= w_i^\top H_i(\lambda)^{-1} H_{h,i} H_i(\lambda)^{-1} w_i \end{aligned} \quad (37)$$

As will be clear in the sequel, the properties of this function $q_i(\lambda)$, which will be called i -th q-function (associated to the i -th barrier), play a key role in our analysis. Note also that every positive $\lambda^* \notin S_{H_i}$ satisfying $q_i(\lambda^*) = 1$ corresponds to a non-degenerate solution, with corresponding equilibrium point given by $x^* = v_i(\lambda^*) + x_i$.

Theorem 4 (Properties of the q-function.). *Let $q_i(\lambda)$ be given by (37), where $H_i(\lambda) = \lambda H_{h,i} - H_V$ is a real symmetric matrix pencil with real spectrum S_{H_i} , associated to the i -th barrier $h(x, \Pi_{h,i})$. Then:*

4.1) If the CLF global minimum $x_0 \in \mathbb{R}^n$ is contained in the safe set, that is, $x_0 \in \mathcal{C} = \bigcap_{i=1}^N \mathcal{C}_i \subset \mathbb{R}^n$ (Assumption II.2), then $q_i(0) \geq 1$.

4.2) If $H_{h,i}$ is invertible, then

$$\lim_{\lambda \rightarrow \pm\infty} q_i(\lambda) = 0. \quad (38)$$

4.3) If $z_{i,k}^\top w_i \neq 0$ for all pencil eigenvectors $z_{i,k} \in \mathbb{R}^n$, we have

$$(i) \lim_{\lambda \rightarrow \lambda_k} q_i(\lambda) = +\infty \quad \forall \lambda_k \in S_{H_i}^+, \quad (39)$$

$$(ii) \lim_{\lambda \rightarrow \lambda_k} q_i(\lambda) = -\infty \quad \forall \lambda_k \in S_{H_i}^-. \quad (40)$$

4.4) If $H_i(\lambda)$ is positive (negative) definite at some interval, then $q_i(\lambda)$ is strictly decreasing (increasing) on that interval.

4.5) If $H_{h,i} > 0$ ($H_{h,i} < 0$), $q_i(\lambda)$ is convex (concave) on the $n - 1$ intervals separating two successive real pencil eigenvalues of positive (negative) type.

Proof. 4.1) Evaluating (37) at $\lambda = 0$ yields

$$\begin{aligned} q_i(0) &= w_i^\top H_i(0)^{-1} H_{h,i} H_i(0)^{-1} w_i \\ &= (x_0 - x_i)^\top H_{h,i} (x_0 - x_i) \end{aligned} \quad (41)$$

Notice that, using (33), (41) can be written as $q_i(0) = 2h_i(x_0, \Pi_{h,i}) + 1$. Then, $q_i(0) \geq 1$ implies $h_i(x_0, \Pi_{h,i}) \geq 0$, which means that $x_0 \in \mathcal{C}_i$. Then, we conclude that if and only if $q_i(0) \geq 1 \forall i = 1, \dots, N$, then the first part of Assumption II.2 holds, since $x_0 \in \mathcal{C} = \bigcap_{i=1}^N \mathcal{C}_i$.

4.2) If $H_{h,i}$ is invertible, there are no pencil eigenvalues at infinity, and therefore $v_i(\lambda) = H_i(\lambda)^{-1}w_i \rightarrow 0$ as $\lambda \rightarrow \pm\infty$. Then, the expression for $q_i(\lambda)$ at (37) proves (38).

4.3) If the spectrum S_{H_i} is real, then $q_i(\lambda)$ admits the diagonalization as presented in Lemma 2. Then, using (37), $q_i(\lambda)$ can be written as:

$$\begin{aligned} q_i(\lambda) &= (Z_i^\top w_i)^\top \begin{bmatrix} (\lambda I_p - \Lambda_{H_i}^+)^{-2} & 0 \\ 0 & -(\lambda I_{n-p} - \Lambda_{H_i}^-)^{-2} \end{bmatrix} Z_i^\top w_i \\ &= \sum_{\lambda_{i,k} \in S_{H_i}^+} \frac{(z_{i,k}^\top w_i)^2}{(\lambda - \lambda_{i,k})^2} - \sum_{\lambda_{i,k} \in S_{H_i}^-} \frac{(z_{i,k}^\top w_i)^2}{(\lambda - \lambda_{i,k})^2}, \end{aligned} \quad (42)$$

where matrix $Z_i = [z_{i,1} \dots z_{i,n}] \in \mathbb{R}^{n \times n}$ collects the pencil eigenvectors $z_{i,k} \in \mathbb{R}^n$ associated to $H_i(\lambda)$. The first and second sums on the right-hand side of (42) collect the p eigenvalues of positive type and the $n - p$ eigenvalues of negative type of $H_i(\lambda)$, respectively. If $z_{i,k}^\top w_i \neq 0$ for all terms, $q_i(\lambda) \rightarrow +\infty$ as λ approaches any eigenvalue of positive type, proving (39). Similarly, $q_i(\lambda) \rightarrow -\infty$ as λ approaches any eigenvalue of negative type, proving (40).

4.4) The first derivative of $q_i(\lambda)$ with respect to λ is:

$$q_i'(\lambda) = -2 v_{h,i}(\lambda)^\top H_i(\lambda)^{-1} v_{h,i}(\lambda), \quad (43)$$

where $v_{h,i}(\lambda) = H_{h,i} v_i(\lambda) \in \mathbb{R}^n$. To derive (43), we have used the first derivative of (35), yielding $H_i(\lambda) v_i'(\lambda) = -H_{h,i} v_i(\lambda)$, and then the derivative of (37). If the pencil $H_i(\lambda)$ is positive (negative) definite at some interval $\mathcal{I} \subset \mathbb{R}$, then the inverse $H_i(\lambda)^{-1}$ is also positive (negative) definite on

\mathcal{I} . In this case, from (43), $q_i'(\lambda)$ is strictly negative (positive), which makes $q_i(\lambda)$ strictly decreasing (increasing) on \mathcal{I} .

4.5) Differentiating (43), the second derivative of $q_i(\lambda)$ is:

$$q_i''(\lambda) = 6 v_{h,i}(\lambda)^\top H_i^{-1}(\lambda) H_{h,i} H_i^{-1}(\lambda) v_{h,i}(\lambda). \quad (44)$$

To derive (44), we have used the second derivative of (35), yielding $2H_{h,i}v_i'(\lambda) + H_i(\lambda)v_i''(\lambda) = 0$, and then the second derivative of (37). Similarly to (37), (44) shows that $q_i''(\lambda)$ has a similar form than $q_i(\lambda)$, with $H_i^{-1}(\lambda)w_i$ replaced by $\sqrt{6}H_i^{-1}(\lambda)v_{h,i}(\lambda)$. Therefore, one can use the canonical form as in (42) to write:

$$q_i''(\lambda) = \sum_{\lambda_k \in S_{H_i}^+} \frac{(z_{i,k}^\top w_i)^2}{(\lambda - \lambda_k)^4} - \sum_{\lambda_k \in S_{H_i}^-} \frac{(z_{i,k}^\top w_i)^2}{(\lambda - \lambda_k)^4}, \quad (45)$$

Since $H_{h,i} > 0$, there are no pencil eigenvalues of the negative type, and therefore the second sum on the right-hand side of (45) vanishes. Therefore, $q_i''(\lambda)$ is strictly positive on its domain, which is $\mathbb{R} \setminus S_{H_i}$. Then, $q_i(\lambda)$ must be *convex* on the $n - 1$ intervals separating two successive pairs of pencil eigenvalues of positive type. A similar argument can be used to show that $q_i(\lambda)$ must be *concave* on the $n - 1$ intervals separating two successive pairs of pencil eigenvalues of negative type, if $H_{h,i} < 0$. \square

Remark III.2. From Theorem 4.4), $q_i'(\lambda) \neq 0$ for any λ at intervals where $H_i(\lambda)$ is a definite matrix (that is, no critical points of q_i exist on these intervals). These intervals were described in Lemma 3.

Next, we present a corollary of Theorem 3 for the specific family of quadratic CLFs and CBFs that we are considering in this section.

Corollary 2. Let the CLF and CBFs be defined by the family of quadratic polynomials (32)-(33), respectively. Then, any boundary equilibrium point $x^* \in \mathcal{E}_i$ that satisfies the matrix pencil strict inequality $H_i(\lambda_i^*) = \lambda_i^* H_{h,i} - H_V > 0$ is unstable, where $\lambda_i^* > 0$ is the scaling between the two collinear gradients on that equilibrium point, as defined in (6).

Proof. This result follows immediately from Theorem 3 and from the fact that the Hessians of the quadratic CLF and the i -th quadratic CBF are constant positive definite matrices. If the pencil $H_i(\lambda_i^*)$ is positive definite at λ_i^* , that is, $H_i(\lambda_i^*) = \lambda_i^* H_{h,i} - H_V > 0$, then $z^\top H_i(\lambda_i^*)z = z^\top (\lambda_i^* H_{h,i} - H_V)z > 0$ for all $z \in \mathbb{R}^n$, yielding $\lambda_i^* z^\top H_{h,i}z - z^\top H_V z > 0$, or $\lambda_i^* \mathcal{D}_z^2 h_i(x^*) - \mathcal{D}_z^2 V(x^*) > 0$ for all $z \in \mathbb{R}^n$. Then, by Theorem 3, the corresponding equilibrium point is unstable. \square

Next, we present the main result of this section, relating the property of compatibility between a quadratic CLF V and a family of quadratic CBFs $\{h_1, h_2, \dots, h_N\}$ to the number of existing equilibrium solutions and properties of the spectrum of the matrix pencils $H_i(\lambda_i^*)$.

Theorem 5. Consider Assumption II.2 and let the CLF and CBFs be defined by the family of quadratic polynomials (32)-(33), respectively. Then, the CLF V is compatible with the

family of CBFs $\{h_1, h_2, \dots, h_N\}$ if the cardinality of each \mathcal{E}_i defined in (6) is not greater than 1:

$$|\mathcal{E}_i| \leq 1, \quad \forall i = 1, \dots, N \quad (46)$$

Proof. First, note that the pencil eigenvalues are real, since $H_V \in \mathcal{S}_+^n$. Since $H_{h,i} \in \mathcal{S}_+^n$, we have $q_i(\lambda) > 0, \forall \lambda \in \mathbb{R}$. Also, statement 1) from Lemma 3 shows that $H_i(\lambda) > 0$ for $\lambda > \max S_{H_i}$. From Theorem 4.4) and (38), $q_i(\lambda)$ is strictly decreasing for $\lambda > \max S_{H_i}$, going from $+\infty$ to 0, which means that, if Assumption II.2 holds, a single equilibrium solution $q_i(\lambda^*) = 1$ satisfying $\lambda_i^* > \max S_{H_i}$, $\lambda_i^* > 0$ must exist. Then, since $H_i(\lambda^*) > 0$, the corresponding boundary equilibrium point is *unstable* from Corollary 2. If other boundary equilibrium solutions exist, they can only exist in the intervals between pairs of successive pencil eigenvalues. On these regions, the pencil $H_i(\lambda)$ is not definite, and therefore no conclusions can be drawn about the stability of the equilibrium point using Theorem 3. Therefore, condition (46) is *sufficient* to show that no stable boundary equilibria exists. Therefore, by Definition II.4, the CLF V and the CBF family $\{h_1, h_2, \dots, h_N\}$ are compatible if condition (46) is satisfied. \square

C. A Numerical Example

In this section, we present a numerical example with a three dimensional quadratic CLF-CBF pair that illustrates the theoretical developments of the last sections. Consider the following CLF-CBF pair in \mathbb{R}^3 :

$$2V(x, \Pi_V) = \sum_{j=1}^3 \sigma_j x_j^2, \quad (47)$$

$$2h(x, \Pi_{h,i}) = \frac{1}{r^2} \sum_{j=1}^3 (x_j - x_{i_j})^2 - 1. \quad (48)$$

The CLF (47) is a quadratic form with parameters σ_1, σ_2 and σ_3 . The CLF level sets are paraboloids in three dimensions aligned with the main axis of the state space and centered on the origin, while the unsafe set defined by the CBF (48) defines an open ball of radius $r > 0$ centered on $x_i^\top = [x_{i_1} \ x_{i_2} \ x_{i_3}]$. In this particular example, we use the values $\sigma_1 = 1.0, \sigma_2 = 3.0, \sigma_3 = 5.0, r = 1, x_i^\top = [1.0 \ 1.0 \ 0.5]$.

Figure 2(a) shows the CBF boundary (in green) modeling the circular obstacle and the geometry of the CLF level set (in blue) on a particular equilibrium point (in red) of the closed-loop system formed by a general driftless nonlinear system with controller (5). Notice that the gradients ∇V and ∇h are positively collinear on the equilibrium point x^* , defining the orthogonal complement $\text{span}\{\nabla V(x^*, \Pi_V)\}^\perp$ (or $\text{span}\{\nabla h(x^*, \Pi_{h,i})\}^\perp$) at that point. This set is also a tangent plane to the CLF and CBF level sets. Geometrically, the differences of sectional curvatures $\Delta \kappa_i(x^*, z)$ on every direction $z \in \text{span}\{\nabla V(x^*, \Pi_V)\}^\perp \equiv \text{span}\{\nabla h(x^*, \Pi_{h,i})\}^\perp$ are positive, which by Theorem 3 implies that x^* is unstable.

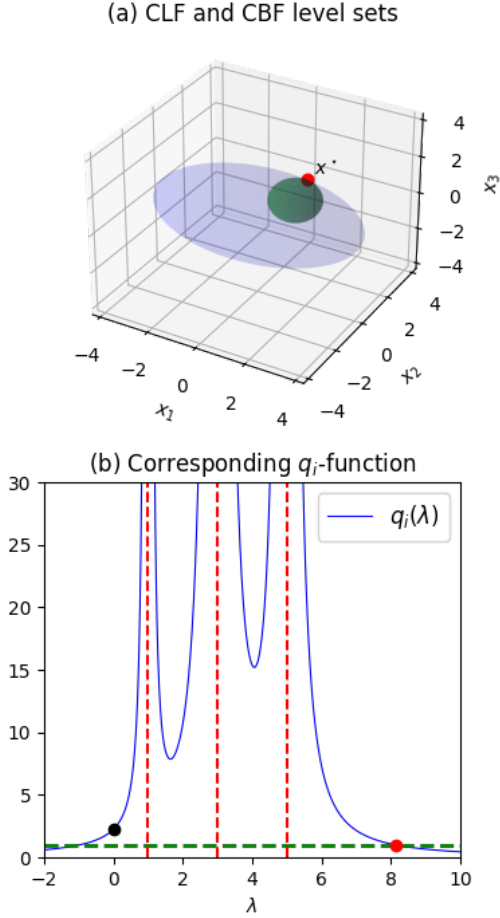


Fig. 2: Example of $q_i(\lambda)$ for $n = 3$: all three pencil eigenvalues are of positive type, there exist two critical points and one unstable equilibrium point.

Using (47)-(48), (35) yields

$$\underbrace{\begin{bmatrix} \lambda - r^2\sigma_1 & 0 & 0 \\ 0 & \lambda - r^2\sigma_2 & 0 \\ 0 & 0 & \lambda - r^2\sigma_3 \end{bmatrix}}_{H_i(\lambda)} \underbrace{\begin{bmatrix} v_{i1} \\ v_{i2} \\ v_{i3} \end{bmatrix}}_{v_i} = r^2 \underbrace{\begin{bmatrix} \sigma_1 x_{i1} \\ \sigma_2 x_{i2} \\ \sigma_3 x_{i3} \end{bmatrix}}_{w_i},$$

Notice that the pencil eigenvalues of $H(\lambda)$ are $\lambda_j = r^2\sigma_j, j = 1, 2, 3$. Furthermore, (36) gives the corresponding q_i -function explicitly as:

$$q_i(\lambda) = \frac{\|v_i(\lambda)\|^2}{r^2} = \sum_{j=1}^3 \frac{(r\sigma_j x_{ij})^2}{(\lambda - r^2\sigma_j)^2} \quad (49)$$

Figure 2(b) illustrates the graph of (49) for the given parameters of the example. Notice that the three pencil eigenvalues are given by $\lambda_1 = 1.0, \lambda_2 = 3.0$ and $\lambda_3 = 5.0$ (vertical red dashed lines), as expected. Notice also that they are all of positive type, due to the positive definiteness of both H_V and $H_{h,i}$. These eigenvalues create a partition of the domain of $q_i(\lambda)$ composed of $n + 1$ open intervals: $\mathcal{I}_1 = (-\infty, \lambda_1)$, $\mathcal{I}_2 = (\lambda_1, \lambda_2)$, $\mathcal{I}_3 = (\lambda_2, \lambda_3)$ and $\mathcal{I}_4 = (\lambda_3, +\infty)$. Notice that $q_i(\lambda)$ is strictly increasing in \mathcal{I}_1 and strictly decreasing in \mathcal{I}_4 , due to the fact that the pencil $H_i(\lambda) < 0$ for $\lambda \in \mathcal{I}_1$ and $H_i(\lambda) > 0$ for $\lambda \in \mathcal{I}_4$, respectively (due to statement 4) of

Theorem 4). Therefore, there exist no critical points of $q_i(\lambda)$ in \mathcal{I}_1 and \mathcal{I}_4 . Since $q_i(\lambda)$ is convex in \mathcal{I}_2 and \mathcal{I}_3 , there exists a single critical point in each one of these intervals.

From (49), notice that $q_i(0) = \|x_i\|^2/r^2$. By Theorem 4.1), the condition $q_i(0) \geq 1$ implies that the origin is contained in the safe set defined by the barrier. Using (49), this condition is equivalent to $\|x_i\| \geq r$, which geometrically means that the origin is not contained inside the ball of radius r that defines the obstacle geometry. From Fig. 2(b), notice that $q_i(0) > 1$ (black point), implying that in fact the obstacle does not enclose the origin for the given parameters of this example.

In general, equilibrium points are computed from $x^* = v(\lambda^*) + x_i$, where λ^* are the positive solutions of $q_i(\lambda^*) = 1$. From (49), these solutions can be computed by finding the roots of a $6n$ -degree polynomial. In Fig. 2(b), only one solution exists (red point) on the interval \mathcal{I}_4 . Since $H_i(\lambda) > 0 \forall \lambda \in \mathcal{I}_4$, the corresponding equilibrium point $x^* = v_i(\lambda^*) + x_i$ is unstable according to Corollary 2. This is precisely the equilibrium point showed in Fig. 2(a). Furthermore, according to Theorem 5, the global minimum of V is the only stable equilibrium point of the closed-loop system resulting from the QP controller (5) with V and $h(x, \Pi_{h,i})$. Therefore, V and barrier h_i are compatible.

In summary, from this example one can see that there is an interesting relation between the geometry of the quadratic CLF-CBF pair and the properties of the q-function. Moreover, the stability analysis of boundary equilibrium points can be simplified considerably by the q-function: in general, using Theorem 5, an n -dimensional quadratic CLF-CBF pair can be proved to be compatible by studying a simple scalar function instead of analysing the spectra of the closed-loop system Jacobian.

IV. LYAPUNOV SHAPING FOR QP-BASED CONTROLLERS

In this section, we seek to design a controller $u^*(x)$ based on the QP formulation (5) that guarantees both stabilization and safety of the trajectories of the feedback system (2), but also ensuring that the CLF V and CBF family $\{h_1, h_2, \dots, h_N\}$ are rendered compatible by using the conditions from Theorem 5.

To this end, we first present the necessary conditions to derive a controller guaranteeing compatibility between a quadratic parametric CLF and the quadratic CBFs. Our objective is to control the CLF parameters in order to guarantee compatibility on the regions where equilibrium points occur in the closed-loop system with controller (5). Finally, the main result of this paper is presented: the design of a controller that dynamically modifies the CLF parameters in (32) in order to guarantee compatibility between the parametric CLF and the CBF family.

A. Guaranteeing Compatibility with Barrier Functions

Assume a given quadratic reference CLF $V(x, \Pi_{V_r})$ and a CBF family $\{h_1, \dots, h_N\}$, both drawn from (32)-(33), respectively. Next, define a quadratic CLF $V(x, \Pi_v)$ with Hessian matrix parameterized by

$$H_V(\pi_v) = L(\pi_v)^T L(\pi_v) + \epsilon_V I_n \in \mathcal{S}^n, \quad (50)$$

where $L : \mathbb{R}^{n(n+1)/2} \rightarrow \mathcal{T}(n)$ is a map from $\mathbb{R}^{n(n+1)/2}$ to the vector space of upper triangular matrices of order n (denoted by $\mathcal{T}(n)$), with dimension $\dim \mathcal{T}(n) = n(n+1)/2$. The parameter vector $\pi_v^\top = [\pi_{v_1} \cdots \pi_{v_{\dim \mathcal{T}(n)}}] \in \mathbb{R}^{\dim \mathcal{T}(n)}$ and a small positive constant $\epsilon_V > 0$ uniquely determine the CLF Hessian matrix H_V , which is positive-definite by construction. Then, the dynamics of (50) is given by:

$$\begin{aligned} \dot{H}_V(t) &= \sum_{j,k=1}^{\dim \mathcal{T}(n)} (\mathcal{T}_j^\top \mathcal{T}_k + \mathcal{T}_k^\top \mathcal{T}_j) \pi_{v_k} \dot{\pi}_{v_j} \in \mathcal{S}^n \quad (51) \\ &= \sum_{j=1}^{\dim \mathcal{T}(n)} \frac{\partial H_V}{\partial \pi_{v_j}} \dot{\pi}_{v_j} \end{aligned}$$

where the \mathcal{T}_j are canonical basis vectors of $\mathcal{T}(n)$. We set $u_v^\top = \dot{\pi}_v^\top = [\dot{\pi}_{v_1} \cdots \dot{\pi}_{v_{\dim \mathcal{T}(n)}}] \in \mathbb{R}^{\dim \mathcal{T}(n)}$ as a control signal designed to control the Hessian matrix H_V .

Considering the i -th barrier h_i , from Lemma (2), the following expressions

$$Z_i^\top H_{h,i} Z_i = I_n \quad (52)$$

$$Z_i^\top H_V Z_i = \Lambda_{H_i}^+ \quad (53)$$

hold for H_V , $H_{h,i}$ and the corresponding pencil eigenvectors of $H_i(\lambda)$. In order to understand the dynamics of the pencil eigenvalues with dynamic changes in the hessian matrices H_V and $H_{h,i}$, we now derive the dynamics of (52)-(53). Taking the time derivative of (52)-(53) and multiplying both sides by $Z_i^{-\top}$ to the left and by Z_i^{-1} to the right yields:

$$H_{h,i} W_i + (H_{h,i} W_i)^\top = -\dot{H}_{h,i} \quad (54)$$

$$H_V W_i + (H_V W_i)^\top = -\dot{H}_V + Z_i^{-\top} \dot{\Lambda}_{H_i} Z_i^{-1} \quad (55)$$

where $W_i = \dot{Z}_i Z_i^{-1}$. Then, matrix W_i maps the pencil eigenvectors $z_{i,k}$ to their respective time derivatives $\dot{z}_{i,k} = W_i z_{i,k}$, ($k = 1, \dots, n-1$). From (55), if $W_i = 0$, the pencil eigenvectors remain constant, yielding $\dot{\Lambda}_{H_i} = Z_i^\top \dot{H}_V Z_i$. Therefore, if and only if $W_i = 0$, the off-diagonal terms of $Z_i^\top \dot{H}_V Z_i$ are zero, which by using (51) yields the following scalar equations

$$\sum_{l=1}^{\dim \mathcal{T}(n)} \left[Z_i^\top \frac{\partial H_V}{\partial \pi_{v_l}} Z_i \right]_{(j,k)} \dot{\pi}_{v_l} = 0. \quad j < k. \quad (56)$$

Equations (56) expresses $\dim \mathcal{S}\mathcal{O}(n) = n(n-1)/2$ linear homogeneous equations in the time derivatives of the CLF parameters. They can be written in matrix form by

$$A_{r,i}(\pi_v) \dot{\pi}_v = 0, \quad (57)$$

where $A_{r,i} : \mathbb{R}^p \rightarrow \mathbb{R}^{\dim \mathcal{S}\mathcal{O}(n) \times \dim \mathcal{T}(n)}$ is a square matrix. Then, if (57) is satisfied, the pencil eigenvectors of $H_i(\lambda)$ remain constant while the geometry of the CLF changes.

Our objective is to control π_v in order to guarantee that the CLF and the CBF family are compatible on the regions where equilibrium points occur.

Corollary 3. Consider Assumption II.2 and let the CLF V be defined by (32) and the CBF family $\{h_1, h_2, \dots, h_N\}$ be defined by (33), for $i = 1, \dots, N$, with the i -th barrier $h_i = h(x, \Pi_{h,i})$. Let $\{\lambda_{i,k}, \lambda_{i,k+1}\}$ be a pair of successive pencil

eigenvalues of $H_i(\lambda) = \lambda H_{h,i} - H_V$. The CLF V and the CBF family $\{h_1, h_2, \dots, h_N\}$ are guaranteed to be compatible if:

$$\log(\sigma_{i,k}^2) - \log(\Delta \lambda_{i,k}^2) > 0, \quad (58)$$

for all $i = 1, \dots, N$ and $k = 1, \dots, n-1$, where $\sigma_{i,k}^2 = \max \left[(z_{i,k}^\top w_i)^2, (z_{i,k+1}^\top w_i)^2 \right]$, and $\Delta \lambda_{i,k} = \lambda_{i,k+1} - \lambda_{i,k}$.

Proof. From Theorem 5, the CLF V and the family of CBFs $\{h_1, \dots, h_N\}$ are compatible if only one equilibrium point exists in each one of the N boundaries. Therefore, if no equilibrium solutions $q_i(\lambda^*) = 1$ exist in the intervals $\mathcal{I}_k = (\lambda_{i,k}, \lambda_{i,k+1})$ ($k = 1, \dots, n-1$), for all $i = 1, \dots, N$, then the CLF and the CBF family are compatible. Since the i -th q-function is convex in each interval I_k , that means that if $q_i(\lambda) > 1$ for $\lambda \in \mathcal{I}_k$ ($k = 1, \dots, n-1$), for all $i = 1, \dots, N$, then the CLF and the CBF family are compatible. In particular, since $q_i(\lambda)$ can be written as (42) (excluding the negative type eigenvalues), where each term is non-negative, one can show that:

$$\frac{(z_{i,k}^\top w_i)^2}{(\Delta \lambda_{i,k})^2} \leq \min_{\lambda \in \mathcal{I}_k} q_i(\lambda), \quad \frac{(z_{i,k+1}^\top w_i)^2}{(\Delta \lambda_{i,k})^2} \leq \min_{\lambda \in \mathcal{I}_k} q_i(\lambda)$$

Then, if the following condition is met:

$$\max \left[\frac{(z_{i,k}^\top w_i)^2}{\Delta \lambda_{i,k}^2}, \frac{(z_{i,k+1}^\top w_i)^2}{\Delta \lambda_{i,k}^2} \right] = \frac{\sigma_{i,k}^2}{\Delta \lambda_{i,k}^2} > 1 \quad (59)$$

for $k = 1, \dots, n-1$ and $i = 1, \dots, N$, then $q_i(\lambda) > 1$ in the intervals $\lambda \in \mathcal{I}_k$, and therefore compatibility is guaranteed. Finally, notice that (58) is simply condition (59) rewritten by taking the natural logarithm on both left-hand and right-hand sides. \square

The next theorem answers the following question: given a family of quadratic CBFs, can some of the CLF parameters in (32) be dynamically modified to satisfy the conditions for compatibility of Corollary 3?

Theorem 6 (Compatible CLF-CBF Controller). Consider the closed-loop system (2), a known reference quadratic CLF $V(x, H_{V_r})$ and a quadratic CLF $V(x, H_V)$, both drawn from (32). Additionally, consider N CBFs $\{h_1, \dots, h_N\}$, each drawn from (33), $i = 1, \dots, N$. Define a Lyapunov function candidate $V_\pi(\pi_v) = \frac{1}{2} \|H_V - H_{V_r}\|_{\mathcal{F}}^2$, where $\|\cdot\|_{\mathcal{F}}$ denotes the Frobenius norm, and $N(n-1)$ barrier candidates for compatibility as

$$h_{\pi_i,k}(\Pi_V, \Pi_{h,i}) = \log(\sigma_{i,k}^2) - \log(\Delta \lambda_{i,k}^2) - \epsilon \quad (60)$$

drawn from condition (58), with $\epsilon > 0$ defined as a small constant. Then, define two QP-based controllers: the first QP

is given by (5). The second QP is defined as:

$$\begin{aligned}
u_v^* &= \underset{(u_v, \delta_v) \in \mathbb{R}^{p+1}}{\operatorname{argmin}} \|u_v\|^2 + p_\pi \delta_v^2 & (61) \\
\text{s.t. } & \langle \nabla_{\pi_v} V_\pi(\pi_v), u_v \rangle + \gamma_\pi V_\pi(\pi_v) \leq \delta_v & (\text{rCLF}) \\
\text{if } x \in \mathcal{S}_i & \begin{cases} \dot{h}_{\pi_{i,1}}(\pi_v, u_v) + \alpha_\pi h_{\pi_{i,1}}(\pi_v) \geq 0 \\ \vdots \\ \dot{h}_{\pi_{i,n-1}}(\pi_v, u_v) + \alpha_\pi h_{\pi_{i,n-1}}(u_v) \geq 0 \\ A_{r,i}(\pi_v) u_v = 0 \end{cases} & (\text{cCBFs})
\end{aligned}$$

where $p_\pi, \gamma_\pi, \alpha_\pi > 0$, and the set \mathcal{S}_i is defined as in (18).

The closed-loop system (2) with control (5) and CLF dynamics (51) with control (61) is safe with respect to \mathcal{C} , and the CLF-CBF pair $\{V, h_i\}$ is rendered compatible in the region \mathcal{S}_i . Furthermore, the CLF $V(x, H_V)$ converges to the reference CLF $V(x, H_{V_r})$ in the region $\overline{\cup_i \mathcal{S}_i} = \cap_i \overline{\mathcal{S}_i}$.

Proof. Initially, by Theorem 1, the first QP-based controller (5) acting on (2) is guaranteed to be feasible on Assumption II.1. Furthermore, it also guarantees that the trajectories are safe with respect to \mathcal{C} . By (61), at any time t_1 , the cCBF constraints are implemented if $x(t_1) \in \mathcal{S}_i$. Therefore, there exists a time $t_2 \geq t_1$ such that $h_{\pi_{i,k}}(t_2) \geq 0, k = 1, \dots, n-1, i = 1, \dots, N$, which means that eventually the conditions (58) of Corollary 3 are guaranteed to be satisfied. Then, the CLF-CBF pair $\{V, h_i\}$ will be rendered compatible at time t_2 : the trajectories will converge towards the CLF minimum, which is guaranteed to be the only stable equilibrium point of the closed-loop system. If the trajectory $x(t) \notin \mathcal{S}_i$ for some t , the only constraint implemented on (61) is the rCLF constraint. Then, the trajectories of the closed-loop system $\dot{\pi}_v = u_v^*$ with controller (61) converge to the state π_{v_r} , which is equivalent to $H_V(\pi_{v_r}) = H_{V_r}$, corresponding to the global minimum of the Lyapunov function $V_\pi(\pi_{v_r}) = \frac{1}{2} \|H_{V_r} - H_V\|_{\mathcal{F}}^2 = 0$. \square

Remark IV.1. The controller proposed in Theorem 6 effectively controls the curvature of the CLF level sets (through the conditions of Theorem 5), in order to achieve compatibility for the CLF-CBF pairs.

B. Compatibility Barrier Dynamics

In (60), the quantities $\sigma_{i,k}^2$ and $\Delta \lambda_{i,k}$ driven from the corresponding q-function $q_i(\lambda)$ are dependent on the CLF and CBF parameters. Therefore, the total time derivative of the compatibility barriers $h_{\pi_{i,k}}(\Pi_V, \Pi_{h,i})$ is dependent on the rate of change of the CLF and CBF parameters. The time derivative of (60) is given by

$$\dot{h}_{\pi_{i,k}} = \frac{\partial h_{\pi_{i,k}}}{\partial t} + \sum_{j=1}^{\dim \mathcal{T}^{(n)}} \frac{\partial h_{\pi_{i,k}}}{\partial \pi_{v_j}} u_{v_j}, \quad (62)$$

$$\frac{\partial h_{\pi_{i,k}}}{\partial t} = \frac{2}{\sigma_{i,k}} z_{i,l}^\top H_V (\dot{x}_i - \dot{x}_0), \quad (63)$$

$$\begin{aligned} \frac{\partial h_{\pi_{i,k}}}{\partial \pi_{v_j}} &= \frac{2}{\sigma_{i,k}^*} \left[z_{i,l}^\top \frac{\partial H_V}{\partial \pi_{v_j}} (x_i - x_0) \right. \\ &\quad \left. - \frac{\sigma_{i,k}^*}{\Delta \lambda_{i,k}} \left(z_{i,k+1}^\top \frac{\partial H_V}{\partial \pi_{v_j}} z_{i,k+1} - z_{i,k}^\top \frac{\partial H_V}{\partial \pi_{v_j}} z_{i,k} \right) \right] \end{aligned} \quad (64)$$

where the l index on $z_{i,l} \in \mathbb{R}^n$ is defined appropriately as $l = \operatorname{argmax}_{k,k+1} [(z_{i,k}^\top w_i)^2, (z_{i,k+1}^\top w_i)^2]$ (l is either k or $k+1$). Equation (62) allows for the computation of the compatibility constraints $\dot{h}_{\pi_{i,k}} + \alpha_\pi h_{\pi_{i,k}}$ in (61).

V. SIMULATION RESULTS

In this section, we present simulation results with the proposed controller for a two-dimensional system, that is, $x = [x_1 \ x_2]^\top$. The proposed CLF is given by

$$V(x, H_V) = \frac{1}{2} \begin{bmatrix} x_1 - x_{01} \\ x_2 - x_{02} \end{bmatrix}^\top \underbrace{\begin{bmatrix} \pi_{v_1} & \pi_{v_2} \\ \pi_{v_2} & \pi_{v_3} \end{bmatrix}}_{H_V} \begin{bmatrix} x_1 - x_{01} \\ x_2 - x_{02} \end{bmatrix} \quad (65)$$

where π_{v_j} are the controlled parameters of the Hessian H_V and $x_0^\top = [x_{01} \ x_{02}]$ is the CLF minimum. The reference Hessian matrix is given by a positive definite matrix H_{V_r} . In these simulations, we proposed three distinct elliptical CBFs with non-intersecting boundaries, each one given by the expression

$$2 h_i(x) = \begin{bmatrix} x_1 - x_{i1} \\ x_2 - x_{i2} \end{bmatrix}^\top \begin{bmatrix} q_{i1}^1 & q_{i1}^2 \\ q_{i1}^2 & q_{i2}^2 \end{bmatrix} \begin{bmatrix} x_1 - x_{i1} \\ x_2 - x_{i2} \end{bmatrix} - 1 \quad (66)$$

with fixed parameters q_{jk}^i for the Hessian $H_{h,i}$ and with $x_i^\top = [x_{i1} \ x_{i2}]$ as their centers.

A. Integrator System

In this section, we present the results obtained for the following integrator system $\dot{x} = u$, where $u = [u_1 \ u_2]^\top \in \mathbb{R}^2$. Each of the quadratic barrier functions corresponds to an ‘‘obstacle’’ represented by the CBF boundaries in Figs. 3-4 (the green ellipses). The CLF level set at some specific given instant is represented by the blue ellipse centered on the CLF minimum, which in this case is the origin ($x_0 = 0 \in \mathbb{R}^2$).

In Fig. 3, we show the results obtained by controller (5). Notice the presence of equilibrium points (red circles) on the obstacle boundaries, computed using the q-functions $q_1(\lambda)$, $q_2(\lambda)$ and $q_3(\lambda)$, each one corresponding to one of the CLF-CBF pairs. Figure 3 also shows the state trajectories and control signal obtained from the simulation: for the given initial condition, the state converges asymptotically to an equilibrium point at the boundary of the rightmost obstacle, modeled by h_3 . In this case, the local curvature $\Delta \kappa_3(x^*, z) = \kappa_{h,3}(x^*, z) - \kappa_v(x^*, z)$ at the equilibrium point x^* is negative for all $z \in \operatorname{span}\{\nabla h_3(x^*)\}^\perp$, which by Theorem 3 means that x^* must be *stable*. Other simulations with different initial states also show the formation and stability of boundary equilibrium points at the top and leftmost obstacles.

In Fig. 4, the results for the proposed compatible CLF-CBF controller presented in Theorem 6 are shown. Here, the reference CLF $V_r = V(x, H_{V_r})$ is the same as the CLF used in the previous simulation. However, the active CLF is given by (65), where the Hessian matrix H_V is controlled by (61), as explained in Theorem 6. By comparing the geometry of the CLF level set in Fig. 4 at $t = 0.2s$ with the one showed in Fig. 3, notice how the proposed controller actively modifies the CLF shape. During this time interval, the third CBF constraint

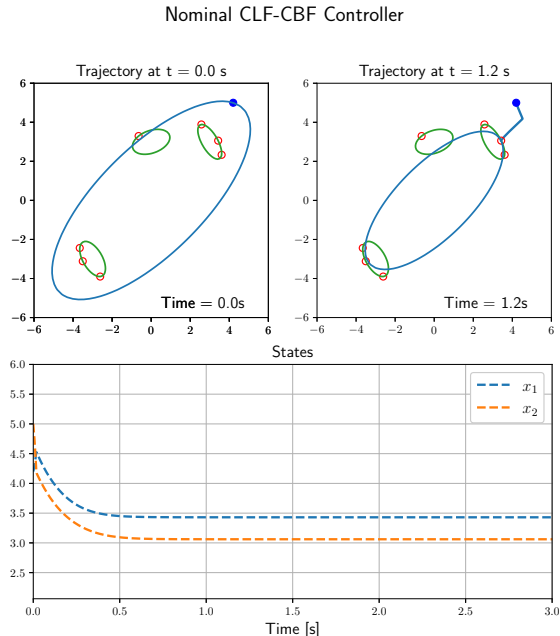


Fig. 3: Results for the nominal QP-based controller proposed by [11]. The ellipses are the CBF boundaries (in green) and the current CLF level set (in light blue), the system trajectory is the light blue curve starting from the dark blue point (initial condition), and the equilibrium points are represented by red circles.

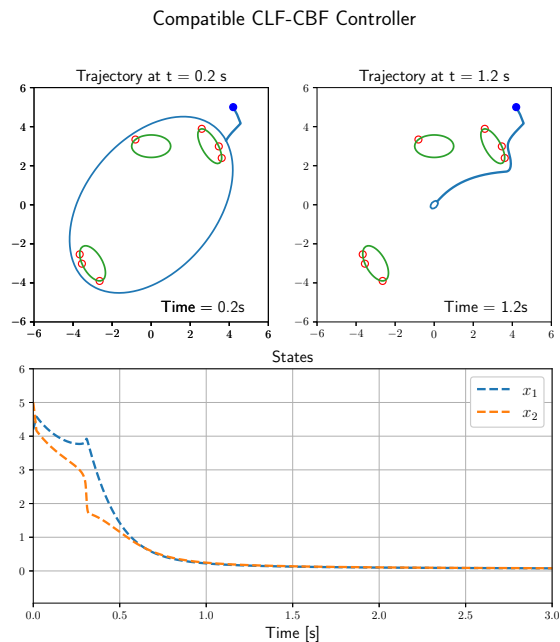


Fig. 4: Results for the proposed controller with compatibility guarantees. The CLF curvature changes dynamically as the trajectory evolves in time, rendering compatibility on the CLF-CBF pairs.

(relative to the rightmost obstacle) in the first QP (5) is the only active CBF constraint ($x(t) \in \mathcal{S}_3$). Therefore, the second QP (61) is implementing the compatibility barrier constraints relative to CBF h_3 , that is, $\dot{h}_{\pi_{3,k}} + \alpha_{\pi} h_{\pi_{3,k}}$, $k = 1, \dots, n-1$. Furthermore, the constraint for pencil eigenvector invariance $A_{r,3} u_v = 0$ is also implemented. Therefore, $V(x, \Pi_V)$ and $h_3(x)$ are eventually rendered compatible, thus guaranteeing that the trajectory is not attracted towards the boundary of the rightmost obstacle. In fact, instead it converges to the origin, under the same initial conditions.

After approximately $t = 1.0s$ of simulation, $x(t) \notin \mathcal{S}_i$, $i = 1, 2, 3$ (no CBF constraint is exclusively active in the first QP), and therefore the CLF shape converges back to the shape of the reference CLF V_r .

B. Path Following with Collision Avoidance

Next, we present the problem of *path following* (PF) control with collision avoidance guarantees. PF control has many of practical applications, such as convoy protection and coordination of robotic swarms, and can be employed with a variety of vehicles such as mobile robots, quadrotors, Underwater Autonomous Vehicles (UAVs), among others [12], [13].

In this proof-of-concept simulation, we consider the application of a drone moving in a plane of constant height, whose navigation objective is to follow a spline-based path while avoiding collisions against three elliptical obstacles intersecting the path, each one modeled by a quadratic barrier function such as (66).

As in the previous simulation, the vehicle model is an integrator $\dot{x} = u$. The proposed quadratic CLF is given by

$$V(x_1, x_2) = \frac{1}{2} e^T H_V(\pi_v) e,$$

where we define the *path following error* as $e = x - x_0(\gamma)$, where $x_0 : \mathbb{R} \rightarrow \mathbb{R}^2$ is a desired parametric spline function of a variable γ , defining a virtual point $x_0(\gamma) \in \mathbb{R}^2$ that moves along the path. Notice that $x_0(\gamma)$ is the CLF global minimum.

Assumption V.1. *The norm of the path gradient $\frac{\partial x_0}{\partial \gamma}$ does not vanish, that is, $\left\| \frac{\partial x_0}{\partial \gamma} \right\| > 0$.*

Using Assumption V.1, the dynamics of the path variable is given by:

$$\dot{\gamma} = \left\| \frac{\partial x_0}{\partial \gamma} \right\|^{-1} \gamma_d, \quad (67)$$

which in turn defines the dynamics of the virtual point, as

$$\dot{x}_0 = \underbrace{\left\| \frac{\partial x_0}{\partial \gamma} \right\|^{-1} \frac{\partial x_0}{\partial \gamma}}_{\hat{\nabla} x_0} \gamma_d,$$

where $\hat{\nabla} x_0$ is the normalized gradient of $x_0(\gamma)$. Then, the speed of the virtual point is given by $\|\dot{x}_0\| = \|\hat{\nabla} x_0\| |\gamma_d| = |\gamma_d|$, showing that γ_d defines the desired speed of the drone along the path.

Figures 5-6 shows the results for path following control with the proposed compatible CLF-CBF controller. Observing the trajectory at $t = 1.92s$ in Fig. 5, the active CLF was initialized

Path Following with Obstacle Avoidance using Compatible CLF-CBFs

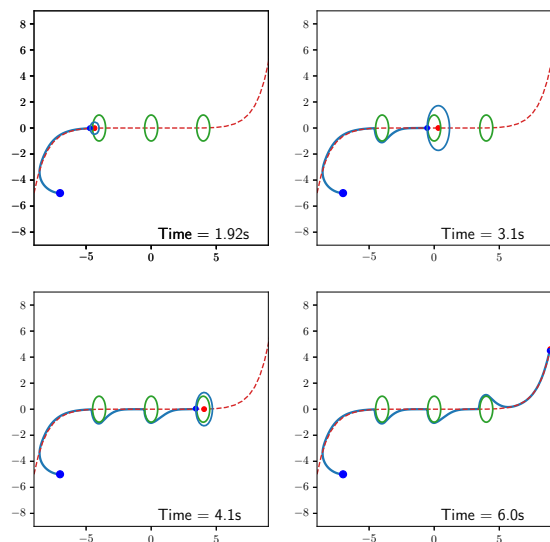


Fig. 5: PF trajectory using the proposed compatible CLF-CBF controller.

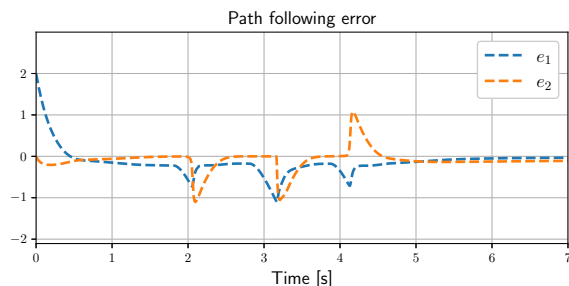


Fig. 6: Path following error using the proposed compatible CLF-CBF controller.

in such a way that an stable equilibrium point would form at the boundary of the first obstacle (from left to right) by using the nominal controller (5), without compatibilization. Therefore, with the nominal controller, the trajectory asymptotically converges to that equilibrium point, and the robot gets stuck in a deadlock configuration as soon as it approaches the leftmost obstacle. Once again, this happens due to the curvature condition (21) not being satisfied on the equilibrium point.

With the proposed compatible CLF-CBF controller, the CLF curvature is dynamically modified by the compatibility barriers in such a way that the stability of this boundary equilibrium point is modified. This way, the trajectory is able to avoid entering the unsafe set while eventually converging back to the virtual point, as it can be seen from Fig. 5 in $t = 3.1s$.

Since the obstacles intersect the path, this process happens three times: every time the robot approaches one of the obstacles. The moments when the CLF is being reshaped by the second QP in (61) are captured in Fig. 5, at times $t = 1.92s$, $t = 3.1s$ and $t = 4.1s$. After $t = 5s$ of simulation, the robot follows the rest of the path with very small error.

Figure 6 shows the path following errors. Notice how the signal peaks three times, precisely at the times when the trajectory is diverging from the path to avoid the obstacles.

Finally, using the proposed compatible CLF-CBF controller from Theorem 6, we were able to design a safe navigation method for a mobile robot that guarantees: (i) quasi-global convergence to the path (deadlock free) and (ii) obstacle avoidance, by using quadratic CLFs and CBFs and the proposed concept of CLF-CBF compatibility.

VI. CONCLUSION

In this work, we have studied the existence and stability of undesirable boundary equilibrium points in the QP framework for safety critical control, for the special class of driftless nonlinear systems and using multiple barrier functions. These equilibrium points arise from gradient collinearity conditions between the CLF and the CBFs used for combining the objectives of (i) stabilization and (ii) safety.

We have shown that, for driftless nonlinear systems, the stability of a boundary equilibrium point is completely determined by the difference of sectional curvatures between the CLF and the corresponding CBF at the equilibrium point. This fact leads to the important concept of *compatibility* between a CLF and a CBF, regarding the number of stable equilibrium points other than the CLF minimum. When applied to the special case of quadratic CLF and CBFs, we have shown that the derived stability condition for boundary equilibrium points can be combined with Matrix Pencil Theory to derive explicit conditions for compatibility between CLF-CBF pairs.

Backed by this theoretical framework, we were able to design a controller that dynamically modifies the shape of the CLF, enforcing these compatibility conditions at the regions of the state space where the undesirable equilibrium points occur. Therefore, the proposed controller is able to achieve: (i) multiple safety guarantees by means of the family of CBFs and (ii) quasi-global convergence of the state trajectories to the CLF minimum, by dynamically reshaping the CLF parameters in order to satisfy the compatibility conditions. Numerical simulations have illustrated these theoretical developments by means of examples and have shown the reliability of the proposed method and its applicability for real engineering applications.

REFERENCES

- [1] L. Lamport, "Proving the correctness of multiprocess programs," *IEEE transactions on software engineering*, no. 2, pp. 125–143, 1977.
- [2] B. Alpern and F. B. Schneider, "Defining liveness," *Information processing letters*, vol. 21, no. 4, pp. 181–185, 1985.
- [3] A. D. Ames, S. Coogan, M. Egerstedt, G. Notomista, K. Sreenath, and P. Tabuada, "Control barrier functions: Theory and applications," *arXiv preprint arXiv:1903.11199*, 2019.
- [4] H. K. Khalil and J. W. Grizzle, *Nonlinear systems*. Prentice hall Upper Saddle River, NJ, 2002, vol. 3.
- [5] A. D. Ames, J. W. Grizzle, and P. Tabuada, "Control barrier function based quadratic programs with application to adaptive cruise control," in *53rd IEEE Conference on Decision and Control*. IEEE, 2014, pp. 6271–6278.
- [6] M. F. Reis, A. P. Aguiar, and P. Tabuada, "Control barrier function-based quadratic programs introduce undesirable asymptotically stable equilibria," *IEEE Control Systems Letters*, vol. 5, no. 2, pp. 731–736, 2021.

- [7] G. Notomista and M. Saveriano, "Safety of dynamical systems with multiple non-convex unsafe sets using control barrier functions," *IEEE Control Systems Letters*, vol. 6, pp. 1136–1141, 2022.
- [8] H. K. Khalil, *Nonlinear systems; 3rd ed.* Upper Saddle River, NJ: Prentice-Hall, 2002.
- [9] P. Lancaster and Q. Ye, "Variational properties and rayleigh quotient algorithms for symmetric matrix pencils," in *The Gohberg Anniversary Collection*. Springer, 1989, pp. 247–278.
- [10] B. N. Parlett, "Symmetric matrix pencils," *Journal of Computational and Applied Mathematics*, vol. 38, no. 1-3, pp. 373–385, 1991.
- [11] A. D. Ames, X. Xu, J. W. Grizzle, and P. Tabuada, "Control barrier function based quadratic programs for safety critical systems," *IEEE Transactions on Automatic Control*, vol. 62, no. 8, pp. 3861–3876, Aug 2017.
- [12] R. P. Jain, A. P. Aguiar, and J. B. de Sousa, "Cooperative path following of robotic vehicles using an event-based control and communication strategy," *IEEE Robotics and Automation Letters*, vol. 3, no. 3, pp. 1941–1948, July 2018.
- [13] M. Reis, R. P. Jain, A. P. Aguiar, and J. Sousa, "Robust moving path following control for robotic vehicles: Theory and experiments," *IEEE Robotics and Automation Letters*, pp. 1–1, 2019.